

Plasma metabolomic study on the effect of *Para*-hydroxybenzaldehyde intervention in a rat model of transient focal cerebral ischemia

XINGLIN YU, YUAN LUO, LIPING YANG and XIAOHUA DUAN

Yunnan Key Laboratory of Dai and Yi Medicines, Yunnan University of Chinese Medicine,
Kunming, Yunnan 650500, P.R. China

Received January 11, 2023; Accepted June 28, 2023

DOI: 10.3892/mmr.2023.13111

Abstract. *Gastrodia elata* Blume has been widely used to treat various central and peripheral nerve diseases, and Para-hydroxybenzaldehyde (PHBA) is one of the indicated components suggested to provide a neuroprotective effect. In our previous, it was shown that PHBA protected mitochondria against cerebral ischemia-reperfusion (I/R) injury in rats. In the present study, how PHBA regulated the metabolic mechanism in blood following cerebral I/R was assessed to identify an effective therapeutic target for the prevention and treatment of ischemic stroke (IS). First, a rat model of cerebral ischemia-reperfusion injury was established via middle cerebral artery occlusion/reperfusion (MCAO/R). The therapeutic effect of PHBA on brain I/R was evaluated by assessing the neurological function score, triphenyl tetrazolium chloride, hematoxylin and eosin, and Nissl staining. Next, a non-targeted metabolomic based on high-performance liquid chromatography quadrupole time-of-flight mass spectrometry was established to identify differential metabolites. Finally, a targeted metabolic spectrum was analyzed and the potential therapeutic targets were verified by Western blotting. The results showed that the neurological function score, cerebral infarction area, hippocampal morphology, and the number of neurons in the PHBA group were significantly improved compared with the model group. Metabonomic analysis showed that 13 different metabolites were identified between the model and PHBA group, which may be involved in the 'tricarboxylic acid cycle', 'glutathione metabolism', and 'mutual transformation of pentose and glucuronates', amongst others. Among these, the levels of the most significant differential metabolite, dGMP, decreased significantly following

PHBA treatment. Western blotting was used to verify the expression of membrane-associated guanosine kinase PSD-95 and the subunit of glutamate AMPA receptor GluA1, which significantly increased after PHBA treatment. In addition, it was also found that PHBA increased the expression of the light chain-3 protein and autophagy effector protein 1, whilst the expression of sequestosome-1 decreased, indicating that PHBA promoted autophagy. Similarly, in TUNEL staining and detection of apoptosis-related proteins, it was found that MCAO/R upregulated the expression of Bax and cleaved-caspase-3 whilst downregulating the expression of Bcl-2 and increasing the apoptosis of hippocampal neurons; PHBA reversed this situation. These results suggest that cerebral I/R causes postsynaptic dysfunction by disrupting the interaction between PSD-95 and AMPARs, and the inhibition of the autophagy system eventually leads to the apoptosis of hippocampal neurons.

Introduction

Stroke remains one of the leading causes of morbidity and mortality, according to the 2022 Global Stroke Survey released by the World Stroke Organization (1). In particular, ischemic strokes (IS) accounts for 70% of all strokes. In general, cerebral ischemia-reperfusion (I/R) injury is a transient or permanent decrease in cerebral blood flow caused by thromboembolic artery occlusion (2). When blood is restored to ischemic tissue, oxidative stress injury and cell death associated with autophagy, necrosis, and apoptosis may occur (3). Although the treatment window for mechanical thrombectomy has increased from a maximum of 6 to ≥ 24 h in the past decade, no post-stroke drug treatments have been developed that can effectively enhance nerve repair and recovery (4). Therefore, blood or brain biomarkers and novel therapies are urgently needed to predict the prognosis of stroke.

Para-hydroxybenzaldehyde (PHBA) is a neuroprotective component of *Gastrodia elata* Blume and has neuroregulatory activity (5). Given its fat solubility and small molecular properties, PHBA can penetrate the blood-brain barrier (BBB) and is used for the treatment of central nervous system injury caused by cerebral ischemia reperfusion (6,7). Additionally, studies have shown that PHBA can protect against brain I/R injury

Correspondence to: Dr Xiaohua Duan, Yunnan Key Laboratory of Dai and Yi Medicines, Yunnan University of Chinese Medicine, 1,076 Yuhua Road, Chenggong, Kunming, Yunnan 650500, P.R. China
E-mail: 1047896527@qq.com

Key words: ischemic stroke, P-hydroxybenzaldehyde, metabolomics, autophagy, apoptosis, PSD-95

and antioxidant stress (7) and reduce inflammatory nerve injury (5). Interestingly, PHBA has a protective effect against ischemic neuronal death in the hippocampal CA1 region and can increase the survival rate of neurons (8). Pharmacokinetics analysis showed that the half-life of PHBA (400 mg/kg) metabolites was significantly prolonged in a model of middle cerebral artery occlusion/reperfusion (MCAO/R) (9). Additionally, our previous study showed that PHBA regulated the expression of apoptosis-related proteins in IS rats, improved mitochondrial oxidative stress and dysfunction, and thus played a neuroprotective role (10). The aim of the present study was to further explore how PHBA regulated the metabolic mechanisms in the blood after brain I/R to identify an effective therapeutic target for the prevention and treatment of IS.

In recent years, metabonomics has received increased attention. By analyzing metabolites *in vivo* by liquid chromatography-mass spectrometry (LC-MS), researchers can associate genotypes with phenotypes and identify biomarkers, thus enhancing the understanding of the brain I/R damage process at the molecular level (11,12). Metabonomics combined with pharmacological verification is an advanced method for the qualitative study of several target compounds of traditional Chinese medicines and has been successfully used to evaluate the overall therapeutic effects of these medicines (13,14). Therefore, this study used liquid chromatography quadrupole time-of-flight mass spectrometry (LC-QTOF/MS) technique to explore the therapeutic mechanism of PHBA for brain I/R injury in rats, with the aim of identifying potential disease biomarkers and highlighting novel approaches for the prevention and treatment of IS.

Materials and methods

Animals. A total of 48 male, pathogen-free, Sprague-Dawley rats (15) [8-12 weeks old, 180-220 g in weight, provided by Changzhou Cavens Experimental Animal Co., Ltd.; laboratory animal certificate no. SCXK (Su) 2021-0013] were used in the present study. Rats were raised in a specific pathogen-free environment maintained at a temperature of 21-25°C and relative humidity of 40-60%, and rats were provided *ad libitum* access to food and water. All animal experiments were approved by the Animal Ethics Committee of Yunnan University of Traditional Chinese Medicine (approval no. R-062019039). All rats were handled according to the Guidelines for the *Care and Use of Laboratory Animals* of the National Institute of Health (16). Before the experiments, the rats were randomly divided into a sham group (Sham), a model group (MCAO/R), or a PHBA group (MCAO/R+PHBA) with 18 rats per group. PHBA ($\geq 98\%$ purity) was purchased from Chengdu Alpha Biotechnology Co., Ltd. According to our previous study (17) the effective dose for the treatment group was 20 mg/kg PHBA and via gavage for 7 days, while the model and Sham groups were administered an equivalent volume of distilled water.

Establishment of the rat model of MCAO/R. Although the risk factors for stroke in older rats are similar to those in humans (15), aged rats were excluded due to anatomical/pathological changes such as middle cerebral artery and common carotid artery aberrations and luminal stenosis (15). Based on a previous preparation method (10), emboli were prepared using a 0.26 mm in diameter nylon thread (Ruibo Biotechnology Co.,

Ltd.), and then placed in heparin sodium (cat. no. 152104037A; Qianhong Biopharma Co., Ltd.). The rats were anesthetized with a small animal anesthesia machine (ZS-MV-IV; Beijing Zhongshidichuang Science and Technology Development Co., Ltd.) using 5% isoflurane (RWD Life Science Co., Ltd.) and maintained with 3% isoflurane, and fixed in the supine position on the experimental table.

The left common carotid artery (CCA) was isolated under a stereomicroscope through a median cervical incision. The left external carotid artery (ECA) and internal carotid artery (ICA) were separated upward, and the two external carotid artery branches of the superior thyroid artery and occipital artery were ligated to reduce the error of thread insertion. The ECA was doubly ligated at 5-8 mm from the near CCA bifurcation and occluded with a micro artery clip at the proximal ends of the ICA and CCA. A 0.2 mm diameter V-shaped microincision was made at the proximal ligation of the ECA. After the nylon thread bolt was gently inserted, the nylon thread was tightened, the artery clamp was loosened, and the nylon thread was moved into the brain along the ECA via the ICA. The insertion depth was 18-20 mm and insertion was halted if slight resistance was felt. The head end of the nylon thread was used to block the blood flow of the MCA. Then, the incision was sutured, and the ischemia time was recorded. After 2 h, the slow and light pulling of the bolt caused the head end to return the CCA, at which point the cerebral I/R was considered to be realized. Samples were obtained from the rats 24 h after reperfusion. In the Sham group: the carotid artery was exposed and isolated without I/R. The body temperatures of all rats were maintained at 37°C throughout the procedure. During this time, none of the animals exhibited symptoms that would require termination, such as not eating, breathing difficulties, convulsions, or hypothermia, nor did any die prematurely. All rats in the study were euthanized before the end of the study.

Neurological function score. After 24 h, the degree of neurological deficit was evaluated using a score of 0-4 (18) as follows. 0, no neurological deficit; 1, left forelimb flexion when lifting the tail in the air; 2, rats walked in circles; 3, hemiplegia causing rats to crawl; and 4, rats were unable to walk spontaneously and had a decreased level of consciousness. A higher score indicated a more serious behavioral disorder.

TTC staining. A total of 24 h after brain I/R, rats were injected intraperitoneally with 2% pentobarbital sodium (150 mg/kg) to induce deep anesthesia. After no response to a tail clip, the rats were euthanized by decapitation, and death was confirmed by a lack of response to tail clamping. The brain was frozen at -20°C for 20 min. The brain was sectioned from front to back with 2 mm coronal sections on ice, stained with 2% TTC staining solution at 37°C for 20 min, and then fixed in 4% paraformaldehyde at room temperature for 24 h. The experimental results were analyzed using ImageJ version 1.52a (National Institutes of Health) software to obtain the total infarcted area and the total area of brain slices. The infarct rate (%) was calculated as the total infarct area/total area of brain slices.

Hematoxylin and eosin (H&E) staining. H&E staining was used to show the components of cytoplasm, muscle fibers, and the general morphological structure of lesions. Nissl is an important

structure involved in protein synthesis in neurons. When neurons are stimulated, the Nissl bodies in the cell become disordered and crumpled. Therefore, detection using H&E staining and Nissl staining provides mutual verification of the pathological injury status of brain tissue (19). Brain tissue sections embedded in paraffin (thickness 5 μm , $n=3$) were heated at 60°C for 3 h, stained with a hematoxylin (using an H&E staining kit; cat. no. KGA224; Nanjing KeyGen Biotech Co., Ltd.) for 2 min, and then washed. Eosin staining was performed for 1 min at room temperature. The samples were dehydrated using a gradient of alcohol solutions, made transparent using xylene, and then sealed with neutral gum. An inverted bright field phase contrast microscope (IX83, Olympus Corporation) was used to obtain the hippocampal images. Fields of view were randomly selected and images were taken at a magnification of x400, and the images were analyzed using ImagePro Plus version 6.0 (Media Cybernetics, Inc.).

Nissl staining. Brain tissue sections embedded in paraffin (thickness 5 μm , $n=3$) were dewaxed, incubated in Nissl staining solution (cat. no. G1430; Beijing Solarbio Science & Technology Co., Ltd.) at 50–60°C for 40 min, washed with deionized water and differentiated using the included differentiation solution. Then, anhydrous ethanol was used for dehydration, xylene was used to clear the tissue, and neutral gum was used for sealing. Images of randomly selected fields of view of the hippocampus were obtained using a phase contrast microscope at a magnification of x400 and were analyzed using ImagePro Plus 6.0 (Media Cybernetics, Inc.).

Sample collection. Whole blood was collected with a heparin sodium anticoagulant tube and centrifuged at room temperature at 3,000 \times g for 10 min. After the blood cells settled entirely to the bottom of the tube, the upper plasma was taken. Plasma (50 μl) from the model group and PHBA group was added to a methanol solution containing an internal standard (4-chlorophenyl alanine, 1 $\mu\text{g}/\text{ml}$) and was then shaken, mixed for 5 min, and centrifuged at 4°C (14,200 \times g for 10 min). The supernatant (200 μl) was transferred to a centrifuge tube and dried using a vacuum drier. The supernatant was then redissolved in 100 μl ultra-pure water and methanol (1:1) and centrifuged at 4°C (14,200 \times g for 10 min). The supernatant volume was 80 μl , and the sample volume injected was 5 μl .

Metabonomics analysis. The LC-QTOF/MS conditions were: Waters HSS T3 1.8 μm , 2.1 \times 100 mm column; flow rate, 0.3 ml/min; column temperature box, 40°C; mobile phase, water phase (ultra-pure water + 0.1% formic acid); B organic phase (acetonitrile). The mass spectrometry conditions were: Mass detection was performed in the positive ion (4,000 V) and negative ion (-4,500 V) mode, respectively, and scanned using a Turbo V electrospray ionization (ESI). The parameters were set as follows: Ion spray voltage, 7 kV; turbine spray temperature, 500°C; declustering potential, 70 V; collision energy, 30 eV; atomizer gas, 55 psi; heater gas, 55 psi; curtain gas, 35 psi. The atomizer and auxiliary gas are maintained by nitrogen. The scanning range of the TOF MS was mCompz 100–1,200.

Total ion chromatographic (TIC) flow analysis of Quality Control (QC) samples. Taking the mixed solution as the QC

sample, in the process of instrumental analysis, a quality control sample was inserted every 10 tests and analysis samples. Through the overlapping display and analysis of the TIC chromatogram of the essential spectrum detection and analysis of the same quality control sample, the stability of the instrument during the testing was judged.

Metabonomics data analysis. The LC-MS data were processed using MS-DIAL (version 5.1.230719) (20). The 'mixOmics' (11) package in R (21) (www.r-project, version 4.2.1) was used for partial least squares discriminant analysis (PLS-DA). The data were unit variance scaled before analysis. The results of the systematic cluster analysis of samples and metabolites are presented as a heat map and tree map generated using the R package 'pheatmap' (11). The variable importance projection (VIP) value was extracted from the PLS-DA results. An unpaired Student's t-test was used to determine the significance. Metabolites that were significantly differentially regulated between groups were determined using the VIP and absolute $\log_2\text{FC}$. The results are presented as a volcanic map ('ggplot2' package) (22). The KEGG database was used to annotate metabolites, which were then mapped to the KEGG pathway database, and the Metaboanalyst website (<http://www.metaboanalyst.ca/>) was used for metabolic pathway analysis. Then, the pathways to which the metabolites with significant regulatory effects were mapped and metabolite concentration were analyzed. The P-value of the hypergeometric test and the size of the pathway influence factors were used to determine the importance of the metabolites.

Western blotting. First, the hippocampal tissues were lysed using RIPA cleavage buffer (PSMF:RIPA lysate=1:100; cat. no. 051021210825; Beyotime Institute of Biotechnology) on ice for 20 min, after which the lysate was centrifuged at 4°C at 13,017 \times g for 5 min. The protein concentration was quantified using a bicinchoninic acid assay. Samples of 80 μg protein were loaded on an 8% SDS gel, resolved using SDS-PAGE at 80 V for ~30 min, followed by 120 V until the target band reached a suitable position. The membrane was then transferred to a PVDF membrane, which was subsequently blocked for 1 h with 5% skimmed milk in TBST at room temperature. Membranes were and then incubated with the primary antibody diluted in TBST solution overnight at 4°C. The primary antibodies used were anti-PSD-95 (1:1,000; cat. no. ab238135; Abcam), anti-Bcl-2 (1:1,000; cat. no. sc-7832; SantaCruz Biotechnology, Inc.), anti-GluA1 (1:1,000; cat. no. 13185; Cell Signaling Technology, Inc.), anti-caspase 3 (1:1,000; cat. no. 9662; Cell Signaling Technology, Inc.), light chain-3 protein, LC3 II/I (1:1,000; cat. no. 4108; Cell Signaling Technology, Inc.), Bax (1:2,000; cat. no. 50599-2-Ig; ProteinTech Group, Inc.), sequestosome-1 (SQSTM1/P62) (1:5,000; cat. no. 18420-1-AP; ProteinTech Group, Inc.), and autophagy effector protein 1 (Beclin1) (1:2,000; 66665-1-Ig; ProteinTech Group, Inc.). The membranes were washed using TBST (0.05% Tween) buffer then incubated with the secondary Goat Anti-Rabbit IgG antibody (cat. no. ab6721) or Rabbit Anti-Mouse IgG (cat. no. ab6728) at room temperature for 1 h (1:10,000; Abcam). Signals were visualized using an ECL kit according to the manufacturer's protocol (Thermo Fisher Scientific, Inc.) and a Tanon 6600 luminous imaging workstation (Tanon Science &

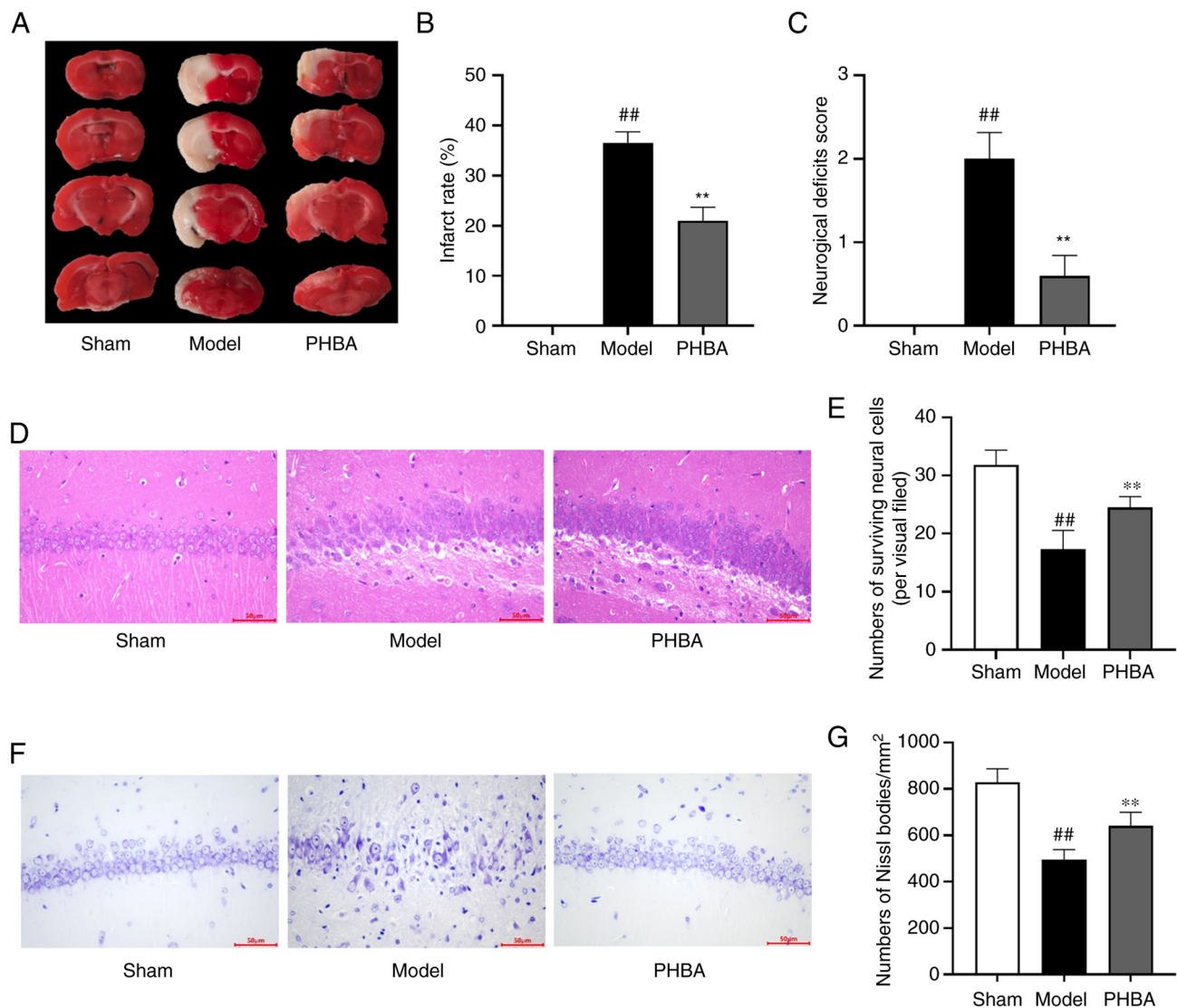


Figure 1. PHBA attenuates the injury of hippocampal neurons in MCAO/R rats. (A) representative images of brain sections stained with TTC. Red, normal tissue; white, infarcted areas. (B) Quantitative analysis of the infarcted size. (C) Neurological deficit scores following 24 h of cerebral I/R. (D and E) H&E staining was used to observe the morphological changes of the hippocampal CA1 region, and quantitative analysis of the numbers of viable neural cells (per visual field). (F and G) Representative images of Nissl staining of hippocampal nerve cells, and quantitative analysis of the numbers of Nissl bodies/mm². All data are represented as the mean \pm the standard error of the mean of three repeats. Magnification, x400; scale bar=50 μ m. ^{##}P<0.01 vs. Sham group; ^{**}P<0.01 vs. Model group. PHBA, P-Hydroxybenzaldehyde; MCAO/R, middle cerebral artery occlusion/reperfusion; I/R, ischemia/reperfusion; H&E, hematoxylin and eosin.

Technology Co., Ltd.). Image ProPlus was used for densitometry analysis.

TUNEL staining. TUNEL staining was performed using a TUNEL detection kit (cat. no. C1090, Beyotime Institute of Biotechnology). After heating at 60°C for 60 min, xylene was used to dewax the brain slices twice, after which samples were hydrated in a series of ethanol solutions (100, 95, 80, and 75%), with 5 min per solution. A total of 20 μ g/ml protease K without DNA enzymes was added to each tissue section and allowed to react at 37°C for 30 min. Subsequently, 50 μ l TUNEL fluorescence detection solution was added to each sample, which was then incubated at 37°C for 60 min, and DAPI double staining was performed at room temperature for 5 min. The hippocampus was observed under a laser confocal microscope (Zeiss LSM). Randomly selected fields of view were captured at x400 magnification.

Statistical analysis. Using GraphPad Prism Version 9.0.0 (GraphPad Software, Inc.) for analysis and processing, if the data were normally distributed and the variance (ANOVA F-test) was uniform, a Bonferroni's multiple comparison test after a one-way ANOVA was used. Data are presented as the mean \pm the standard error. P<0.05 was considered to indicate a statistically significant difference.

Results

PHBA ameliorates brain injury and pathological damage of hippocampal neurons in MCAO/R rats. The results of TTC staining showed that there were notable white infarcted areas following brain I/R. Compared with the model group, PHBA significantly reduced the size of infarct sizes [F (2,6) 1.822, P=0.413] (Fig. 1A and B) and improved the neurological function of rats [F (2,12) 1.333, P=0.300] (Fig. 1C). It has

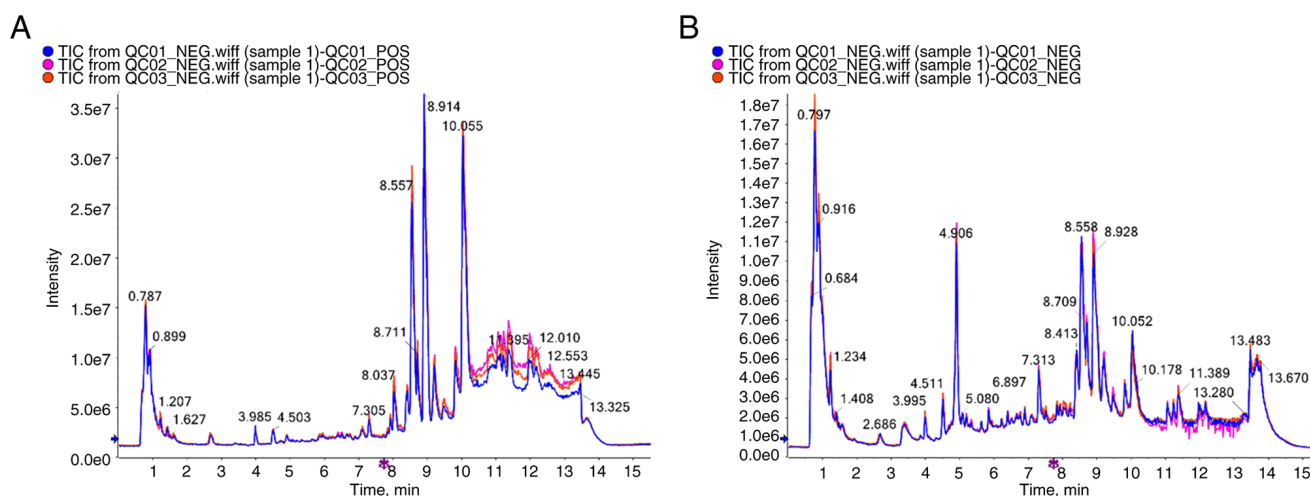


Figure 2. QC sample TIC overlap map. (A) TIC overlap map of QC samples in positive mode. (B) TIC overlap map of QC samples in negative mode. QC, quality control; TIC, total ion chromatographic.

been shown that PHBA can effectively reduce brain injury in MCAO/R rats (10). To further explore the effects of PHBA on the pathological changes of the brain following I/R injury, HE and Nissl staining were used in this study. The results showed that the number of cells [F (2,15) 1.273, $P=0.529$] in the sham group was higher, the nuclei and cell bodies of neurons in the sham group were clear, and the Nissl bodies [F (2,15) 0.121, $P=0.887$] were abundant. Conversely, in the model group, hippocampal ischemic neuronal injury, nuclear pyknosis, a disorderly arrangement of neurons, and sparsity of Nissl bodies were observed. PHBA reversed these changes (Fig. 1D-G). The above data suggest that PHBA had a protective effect on hippocampal neuronal death after I/R.

Screening and identification of differential metabolites between the model and PHBA groups. The high stability of the LC-QTOF/MS instrument provides an essential guarantee for the repeatability and reliability of data. The curve overlaps of the total ion currents of the QC samples were high, suggesting that the experimental data were stable (Fig. 2). To ascertain the changes of metabolites following PHBA treatment, the plasma of rats in the model and PHBA groups ($n=6$) were collected. In addition, based on the LC-QTOF/MS detection platform and database, 856 metabolites were detected under positive and negative ions, including purines, pyrimidines, amino acids, and other metabolites. To further determine the differences between groups, the multivariate statistical analysis method PLS-DA was used to analyze the two groups in pairs. The results showed there was a significant separation between the model and the PHBA group, and the internal correlation between each group was very high (Fig. 3A and B). The screening results are shown as a volcano map (Fig. 3C and D). In addition, the stratified cluster heat map was used to show the changes in metabolites more directly. The heat map showed that the model and PHBA group could be divided into two parts according to the identified metabolites (Fig. 3E and F). Finally, 13 differential metabolites were identified, of which 6 metabolites were upregulated: benzamide, pyroglutamic acid, fumaric acid, d-Xylulose, cholic acid, and cis-Aconitic acid, and 7 metabolites were downregulated: 2'-Deoxyguanosine

5'-monophosphate (dGMP), hexadecanedioic acid, deoxycholic acid, deferoxamine, 4-Nitrophenyl phosphate, bilirubin, leukotriene C4 (Table I). Among these metabolites, the P -value of dGMP was the lowest (0.018).

Enrichment analysis of differential metabolites using KEGG. To comprehensively observe the changes in metabolic pathways, pathway enrichment analysis of all differential metabolites was performed. In positive ion mode, the primary ways that the model group and the PHBA group were affected by the differential metabolites were: The Tricarboxylic acid (TCA) cycle', 'glutathione metabolism', and 'mutual transformation of pentose and glucuronates' (Fig. 4A). This may be related to the improvement of energy metabolism and the antioxidant effect of glutathione metabolic pathway by PHBA, which has been reported in the pathogenesis of glucose metabolic diseases (23). In negative ion mode, the primary pathways affected by the differential metabolites were: The 'TCA cycle' and 'arachidonic acid metabolism', amongst others (Fig. 4B). This suggests that MCAO/R inhibits energy production and induces inflammation. These pathways interact with each other and are closely related to I/R. From the above results, it can be inferred that PHBA components are absorbed into the blood and achieve their neuroprotective effects by regulating various metabolic processes in the body, especially those related to the TCA cycle (Fig. 4C).

Effect of PHBA on the expression of PSD-95 and NMDAR in the hippocampus. The most significantly different metabolite induced by PHBA was dGMP. Guanosine kinase (GK) can phosphorylate dGMP to dGDP as a central enzyme in the guanine rescue pathway (24). The changes in PSD-95 levels in the membrane-associated guanosine kinase (MAGUK) family are related to the content of synaptic AMPAR (GluA1), which regulates the intensity of hippocampal synaptic activity and is associated with neuroplasticity (25). Here, the protein expression levels of PSD-95 and GluA1 were determined. Western blotting results showed that the expression of PSD-95 [F (2,6) 0.035, $P=0.966$] and GluA1 [F (2,6) 1.684, $P=0.263$] increased significantly compared with the model group following PHBA

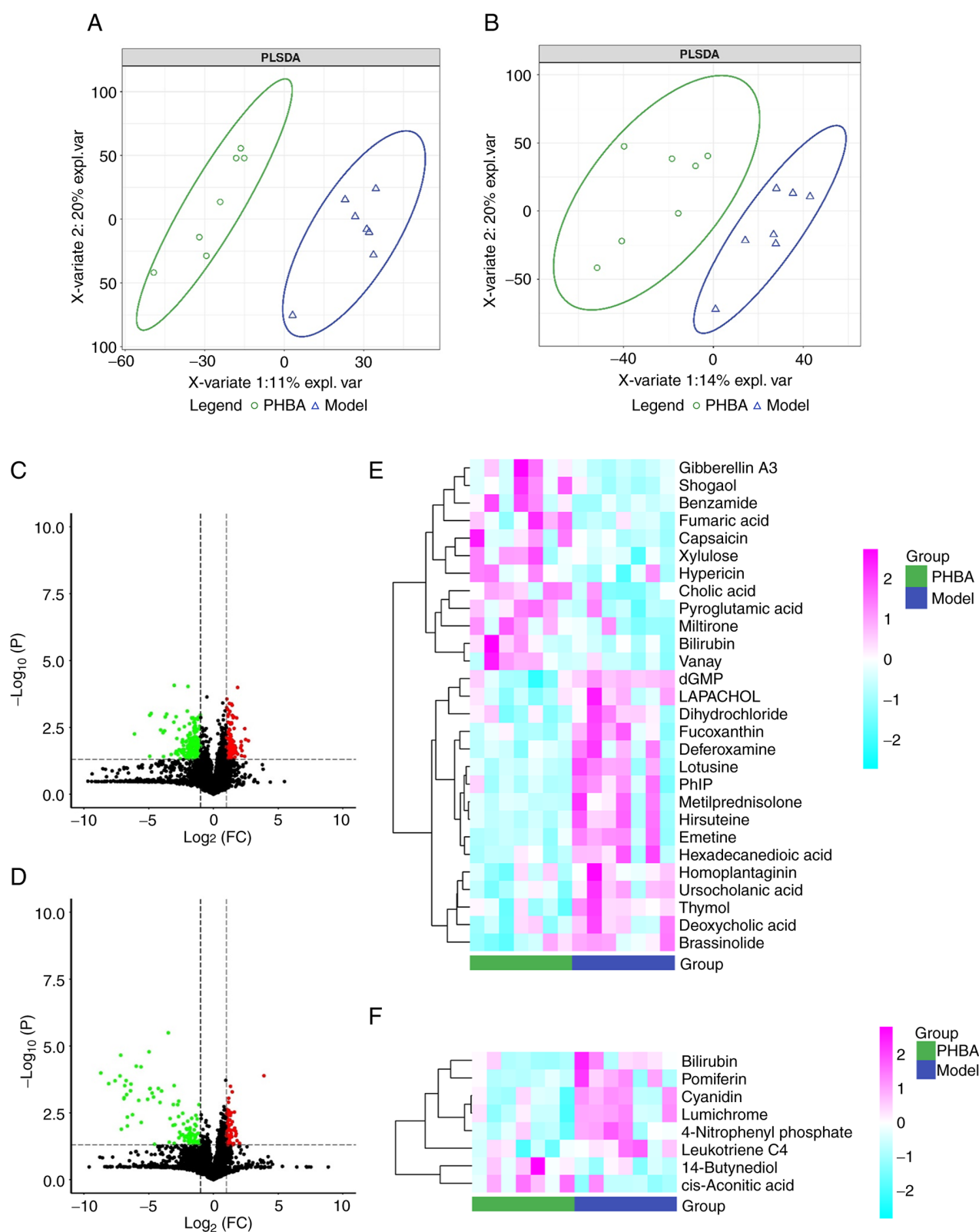


Figure 3. Differential metabolite enrichment analysis between the Model and PHBA group. (A) Enrichment analysis of differential metabolites between the model group and PHBA group PLS-DA score map in positive mode. (B) PLS-DA score diagram in negative mode. (C) Volcano map using the positive model. (D) Volcano map using the negative model. (E) Heat map in the positive mode. (F) Heat map in the negative mode. Pink, highly expressed metabolites; blue, lowly expressed metabolites. PHBA, P-Hydroxybenzaldehyde; PLS-DA, partial least squares discriminant analysis.

treatment (Fig. 5A-C). This suggested that PHBA increased the levels of dGMP in the brain following IS by promoting the interaction between PSD-95 and AMPAR.

Effect of PHBA on autophagy in hippocampal neurons. To verify whether PHBA ameliorates I/R by activating autophagy, western blotting was used to detect the effects of PHBA on

Table I. Screening results of differential metabolites in the Para-hydroxybenzaldehyde group compared with the model group.

Compound	Formula	KEGG	Variable importance projection	Fold change	P-value	Change in expression
dGMP	C ₁₀ H ₁₄ N ₅ O ₇ P	C00362	2.498	1.278	1.76x10 ⁻³	Down
Cholic acid	C ₂₄ H ₄₀ O ₅	C00695	2.132	0.424	1.41x10 ⁻²	Up
Benzamide	C ₇ H ₇ NO	C09815	2.070	0.322	1.65x10 ⁻²	Up
4-Nitrophenyl phosphate	C ₆ H ₆ NO ₆ P	C03360	1.895	1.553	2.36x10 ⁻²	Down
cis-Aconitic acid	C ₆ H ₆ O ₆	C00417	1.887	0.600	2.43x10 ⁻²	Up
Leukotriene C4	C ₃₀ H ₄₇ N ₃ O ₉ S	C02166	1.991	1.303	2.65x10 ⁻²	Down
Bilirubin	C ₃₃ H ₃₆ N ₄ O ₆	C00486	1.991	2.155	2.69x10 ⁻²	Down
Pyroglutamic acid	C ₅ H ₇ NO ₃	C01879	1.942	0.687	2.70x10 ⁻²	Up
D-Xylulose	C ₅ H ₁₀ O ₅	C00310	1.904	0.767	3.20x10 ⁻²	Up
Deferoxamine	C ₂₅ H ₄₈ N ₆ O ₈	C06940	1.913	1.835	3.20x10 ⁻²	Down
Fumaric acid	C ₄ H ₄ O ₄	C00122	1.890	0.646	3.43x10 ⁻²	Up
Hexadecanedioic acid	C ₁₆ H ₃₀ O ₄	C19615	1.874	1.847	3.43x10 ⁻²	Down
Deoxycholic acid	C ₂₄ H ₄₀ O ₄	C04483	1.925	1.319	3.60x10 ⁻²	Down

KEGG, Kyoto Encyclopedia of Genes and Genomes.

the expression of the autophagy marker LC3 and essential autophagy proteins p62 and Beclin1 (Fig. 6A). The results showed that compared with the model group, PHBA significantly increased the expression of LC3-II/LC3I [F (2,6) 0.463, P=0.650] and Beclin1 [F (2,6) 1.730, P=0.255] (Fig. 6B and C), and decreased the protein expression levels of p62 [F (2,6) 0.103, P=0.903] (Fig. 6D). This suggests that autophagy in the hippocampus is significantly activated following PHBA treatment, which may be related to the interaction between PSD-95 and AMPAR.

Effect of PHBA on the apoptosis of hippocampal neurons. It is well-established that brain I/R is often associated with neuronal injury and apoptosis (18,19). TUNEL staining showed that the number of positive cells in the hippocampus of the model group was significantly higher than that of the sham group. After treatment with PHBA, the number of positive cells in the hippocampus decreased significantly [F (2,6) 1.169, P=0.373] (Fig. 7A and B). In addition, the protein expression levels of apoptosis-related genes were analyzed by western blotting (Fig. 7C-G). MCAO/R resulted in the upregulation of Bax [F (2,6) 1.207, P=0.363] and cleaved-caspase-3 [F (2,6) 0.349, P=0.719] expression and downregulation of Bcl-2 [F (2,6) 0.734, P=0.519] expression. However, PHBA partially reversed the MCAO/R-induced apoptosis. These results suggested that PHBA inhibited I/R-induced apoptosis of hippocampal cells and reduced the loss of neurons.

Discussion

Several studies have shown that PHBA has significant potential for treating IS (10,17). However, whether PHBA has a protective effect against brain I/R via regulation of metabolomic characteristics has not been reported previously to the best of our knowledge. To elucidate the therapeutic impact of PHBA for the management of brain I/R injury, metabolomic

analysis and pharmacodynamic experiments were performed, and biochemical and histopathological indices were measured. The results showed that the differential metabolites in plasma exerted a neuroprotective effect against IS via the regulation of numerous metabolic pathways such as energy, glucose, and oxidative metabolism. The results also suggested that interactions between PSD-95 and AMPAR may promote synaptic plasticity in hippocampal neurons and reduce brain damage mediated by autophagy deficiency in MCAO/R rats, thus inhibiting apoptosis of hippocampal neurons. Therefore, PHBA promoted the activity of PSD-95-AMPA and thus played a neuroprotective role.

The results of metabolomics showed the metabolites regulated by PHBA that were involved in brain I/R, which primarily included plasma purines, pyrimidines, and amino acids. The primary pathways these differential metabolites were involved in were the 'TCA cycle', 'arginine biosynthesis', and 'mutual transformation of pentose and glucuronates'. It is worth noting that compared with the model group, PHBA increased the levels of benzamide, pyroglutamic acid, fumaric acid, d-xylulose, cholic acid, and cis-aconitic acid, whilst decreasing hexadecanedioic acid, deoxycholic acid, deferoxamine, 4-nitrophenyl phosphate, bilirubin, leukotriene C4, and dGMP levels.

Benzamides exhibit brain region specificity, can cross the BBB, and increase the levels of histone acetylation in the hippocampal regions involved in behavior and cognition (26). In a model of mouse brain I/R, benzamide treatment significantly reduced the extent of delayed neuronal apoptosis in the hippocampus of mice, thus improving neuronal survival and memory (27). Pyroglutamic acid is an important molecule involved in glutathione metabolism. The decrease in pyroglutamic acid in patients with cerebral infarction indicates a decrease in reducing substances caused by oxidative stress (28,29). D-xylulose is the product of a dehydrogenase reaction when xylitol is used as a substrate. In rat brains,

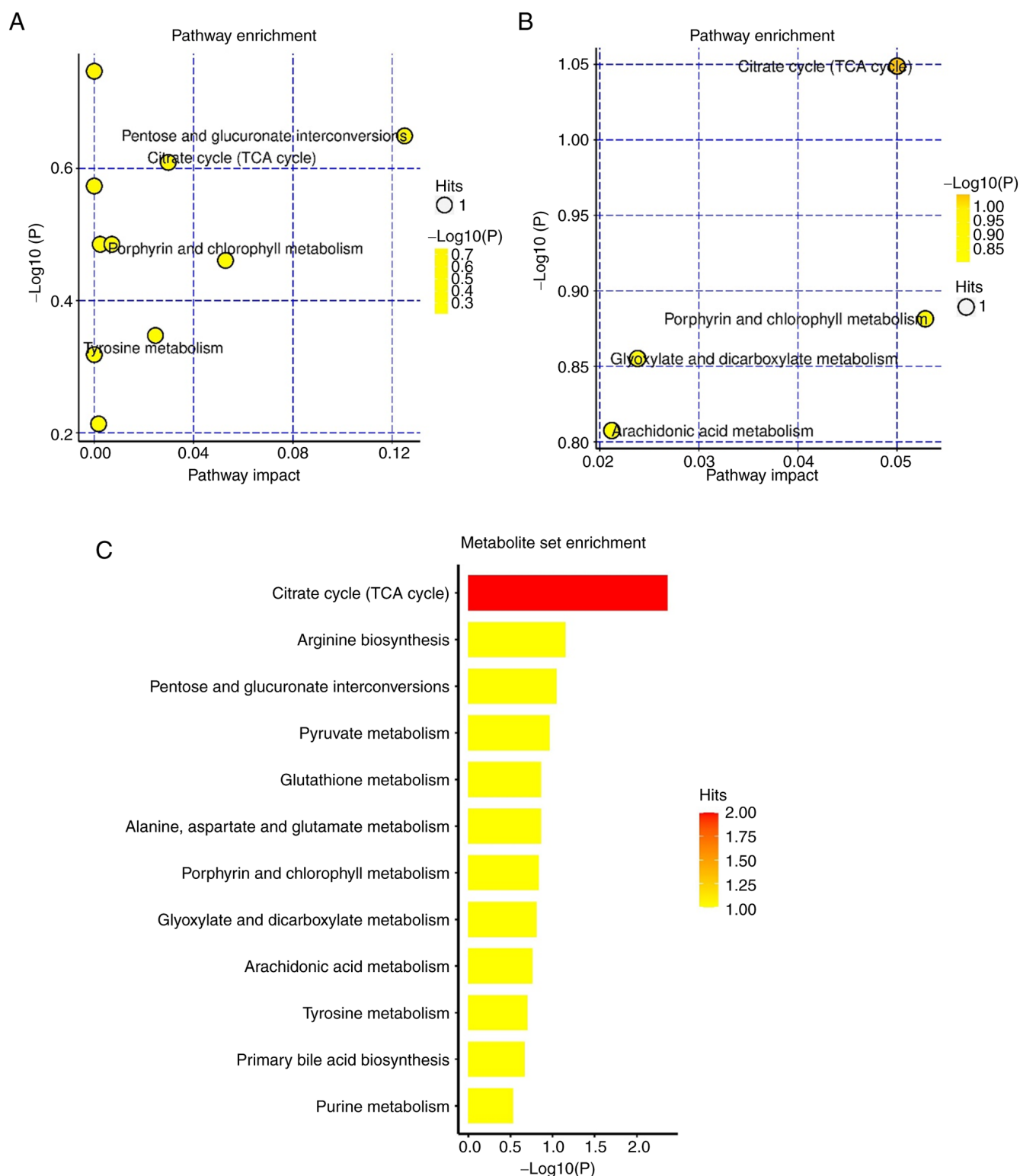


Figure 4. Enrichment analysis of the metabolic pathways in the model group and PHBA group. Bubble diagram of the metabolic pathways in the (A) positive mode and (B) negative mode. (C) The total score map of the differential metabolic pathways. PHBA, P-Hydroxybenzaldehyde; TCA, tricarboxylic acid.

d-xylulose, similar to glucose, stimulates hormone secretion through a nicotinamide nucleotide-dependent mechanism (16). Fumaric acid is the precursor of L-malic acid in the TCA cycle and is formed by the oxidation of succinic acid (30). Cis-aconitic acid is an intermediate of the TCA cycle in mitochondria that is synthesized by aconitase and can affect cell energy metabolism (31). A catalase modified via maleic

anhydride has been developed that can inhibit reactive oxygen species-mediated apoptosis, thereby reducing the cerebral infarction volume of MCAO mice (32). The primary active components of bile acid biosynthesis include cholic acid, deoxycholic acid, and taurine deoxycholic acid (33). Among these, the mechanism of cholic acid in protecting against IS may involve the BDNF-TrkB pathway by protecting the

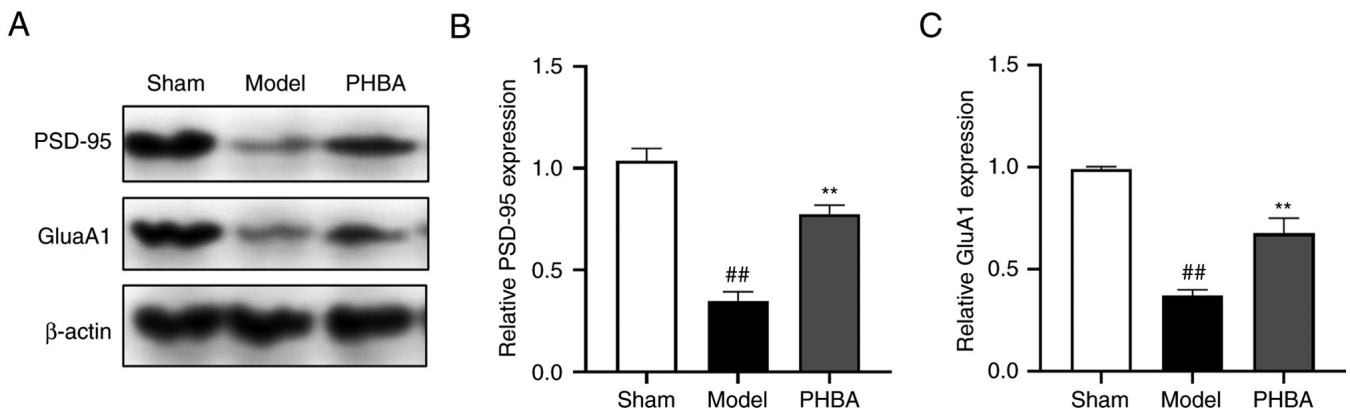


Figure 5. Effect of PHBA on PSD-95 and GluA1 in MCAO/R rats. (A) Representative western blot of PSD-95 and GluA1. Densitometry analysis of (B) PSD-95 and (C) GluA1 expression. All data are presented as the mean \pm the standard error of the mean of three repeats. ## P <0.01 vs. Sham group; ** P <0.01 vs. Model group. MCAO/R, middle cerebral artery occlusion/reperfusion; GluA1, glutamate AMPA receptor 1.

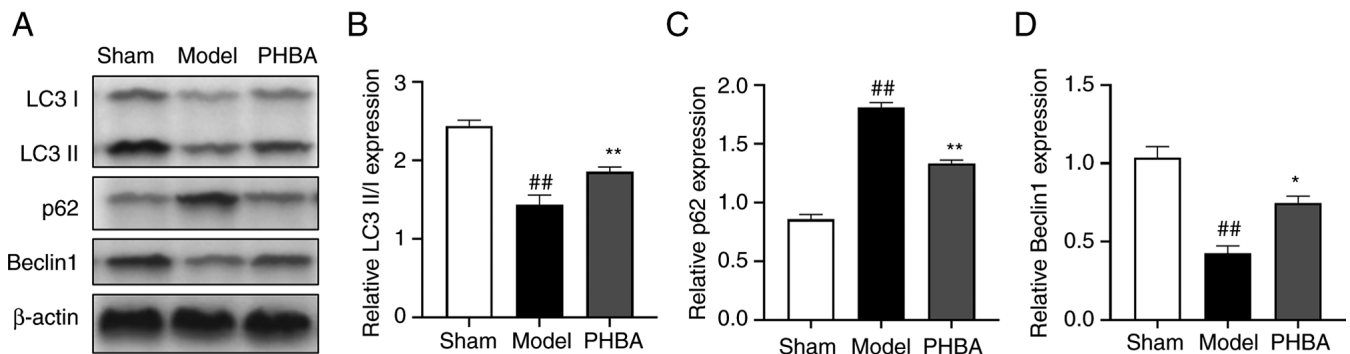


Figure 6. Effect of PHBA on autophagy in the hippocampus of MCAO/R rats. (A) Representative blots of typical autophagy-associated proteins. (B) Quantitative analysis of LC3 II/I expression. (C) Quantitative analysis of p62 expression. (D) Quantitative analysis of Beclin1 expression. Data are presented as the mean \pm the standard error of the mean of three repeats. ## P <0.01 vs. Sham group; * P <0.05, ** P <0.01 vs. Model group. PHBA, P-Hydroxybenzaldehyde; MCAO/R, middle cerebral artery occlusion/reperfusion.

integrity of the BBB of the neurovascular unit BBB *in vitro*, downregulating apoptosis, and finally, reducing the oxidative stress and inflammatory injury of the neurovascular unit following oxygen-glucose deprivation/reoxygenation (34). In contrast, an abnormal increase in the bile acid-related metabolite, deoxycholic acid, significantly affected BBB permeability following brain injury (35). In the present study, deoxycholic acid levels decreased following PHBA treatment, as well as downstream metabolites of molecules affected by PHBA. A previous study reported that hexadecanedioic acid was associated with blood pressure levels and all-cause mortality (36). Sun *et al* (37) performed a metabolomics study of 114 patients with IS and 112 healthy controls. The results showed that the pathways related to intracellular hexadecanedioic acid synthesis were involved in the occurrence of IS. A previous study showed that deferoxamine, an iron-chelating agent, can quickly enter the brain tissue through the BBB to counteract an overload of iron ions in the brain, but it had no effect on the clinical symptoms of IS (38). Bilirubin is the primary product of heme catabolism (39). Its toxicity involves a variety of pathological mechanisms, and neurons and glial cells are susceptible to bilirubin toxicity. Bilirubin also affects brain circuits, particularly those that affect cognition, learning, behavior, and sensation (40). Clinically high serum bilirubin

levels were positively correlated with the severity of IS and the degree of disability 3 months after stroke onset (41). 4-nitrophenyl phosphate is the substrate of alkaline phosphatase and can inhibit the phagocytosis of macrophages in the nervous system (42). Leukotriene C4 is a metabolite of arachidonic acid found in the forebrain (43), and increases in leukotriene C4 in the hippocampus are greatest after I/R. Accumulation of leukotriene C4 may alter the membrane permeability, cause BBB dysfunction and edema, and eventually, neuronal death (44).

It is worth noting that the most significantly differentially expressed metabolite induced by PHBA was dGMP. Deoxyguanosine, in the pathway from exogenous guanine to DNA, can readily produce toxic cellular dGMP (45). Interestingly, the results of the present study showed that PHBA treatment significantly reduced plasma dGMP levels. When further examining the mechanism of dGMP following treatment, it was found that GK could phosphorylate dGMP to produce dGDP, which is a central enzyme in the guanine rescue pathway (24). GK is a domain of the PSD-95 family of membrane-associated guanylate kinases and is largely found in the MAGUK family, especially in neuronal tissues (46). PSD-95 is an important postsynaptic membrane protein involved in synaptic plasticity. It exhibits neuroplasticity and

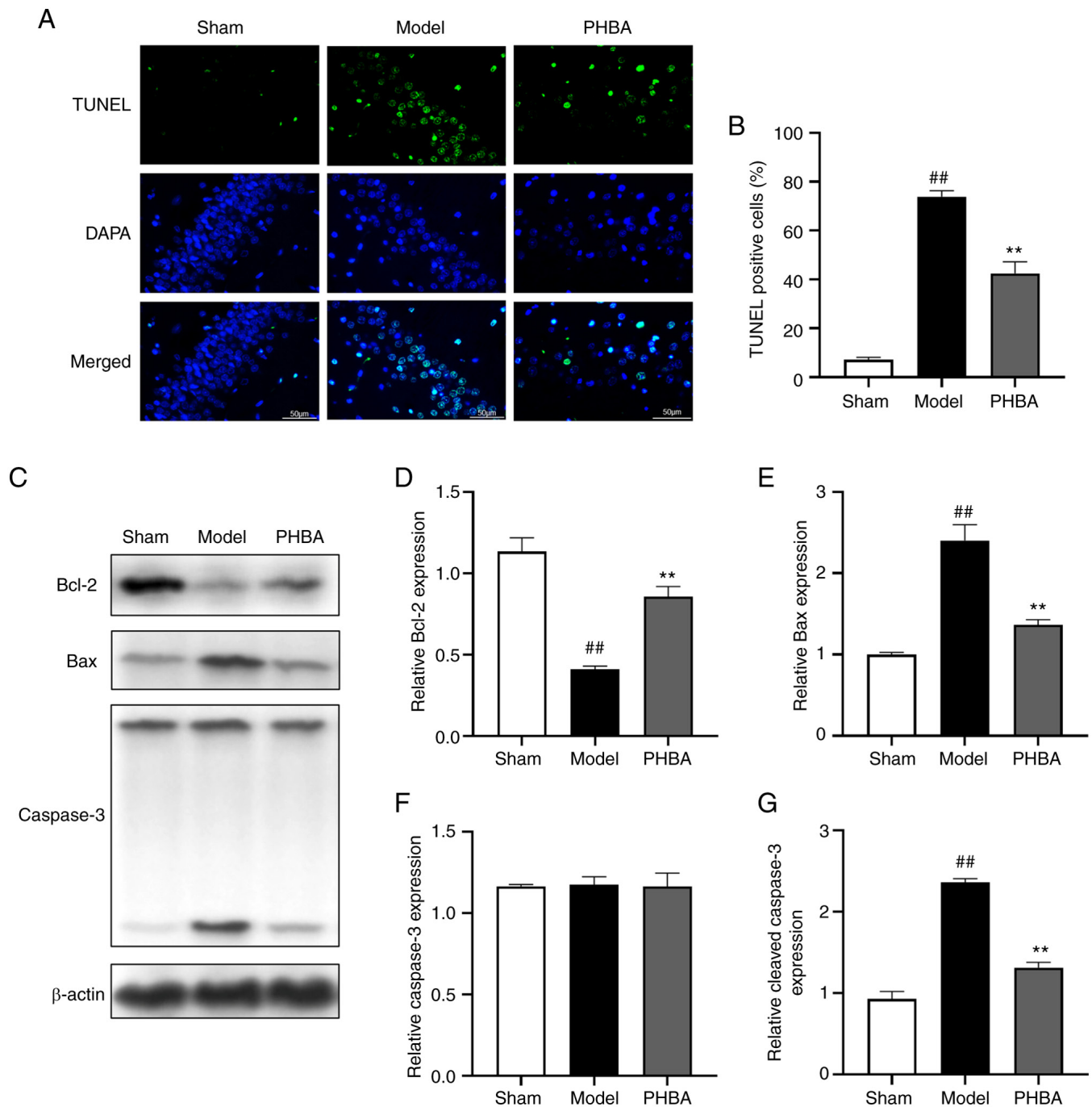


Figure 7. PHBA attenuates MCAO/R-induced apoptosis in the rat hippocampus. (A) TUNEL staining (green) staining and DAPI (blue) staining of nuclei was detected using a fluorescence microscope. (B) Quantitative analysis of the number of apoptotic cells in the hippocampus. (C) Representative blots of apoptosis-related proteins. Densitometry analysis of (D and E) Bcl-2 and Bax expression, and (F and G) caspase-3 and cleaved-caspase-3 expression in the hippocampus. Magnification, x400; scale bar, 50 μ m. All data are presented as the mean \pm the standard error of the mean of three repeats. ^{##} $P < 0.01$ vs. Sham group; ^{**} $P < 0.01$ vs. Model group. PHBA, P-Hydroxybenzaldehyde; MCAO/R, middle cerebral artery occlusion/reperfusion.

contributes to brain repair, thus improving the prognosis of IS (25). In addition, studies have shown that PSD-95 mediates the postsynaptic localization of ~40% of AMPARs (the GluA1 protein is an essential subunit of AMPAR) in hippocampal CA1 pyramidal cells (47). The hippocampal damage caused by I/R leads to cognitive and memory impairment in animals, and the increased expression of PSD-95 is a marker of recovery of neurological function (48). Therefore, it was hypothesized that following cerebral I/R injury, PHBA may accelerate dGMP metabolism by promoting

the interaction between PSD-95 and AMPAR resulting in synaptic structural changes that inhibit the dGMP levels in the plasma following MCAO/R, thus reducing neurotoxicity. Interestingly, the results showed that PHBA significantly increased the protein expression levels of PSD-95 and GluA1 in the hippocampus and decreased the levels of dGMP in the plasma of I/R rats. These results suggested that the neuroprotective effects of PHBA in cerebral I/R injury were associated with promoting synaptic recovery and neural plasticity.

It is well established that structural autophagy is responsible for neuronal survival and protects neurons from nutritional starvation (49-51). There is growing evidence that autophagy provides neuroprotection and improves clinical symptoms by significantly reducing ischemic damage to neurons, glial cells, and endothelial cells (52,53). Several key molecular components are involved in autophagy, such as Beclin1 and LC3 (54), that promote autophagy. In addition, p62, as a selective autophagy substrate, is degraded during autophagy activation (55). It is worth noting that the decreased expression of PSD-95 in hippocampal neurons following experimental brain injury was accompanied by reduced inhibition of LC3-positive autophagosomes and mitochondrial mass, indicating autophagy dysfunction (56). Consistent with previous reports, it was found that the expression of the autophagy markers LC3 and Beclin1 decreased and expression of the autophagy-associated protein p62 increased in the hippocampus of rats in the model group, indicating that autophagy was inhibited. However, this result was reversed following PHBA treatment, suggesting that the potential neuroprotective effect of PHBA in the pathological mechanism of cerebral I/R injury was related to its promotion of autophagy and reduction of ischemic synaptic damage.

Hippocampal neuronal damage caused by apoptosis is the focus of treatment after cerebral I/R injury, therefore, inhibition of apoptosis is a neuroprotective strategy in IS therapy (57). Further analysis of the biological function of PSD-95 and AMPARs showed that the interaction between overexpression of PSD-95 and AMPARs reduced the expression of the pro-apoptotic protein Bax and increased the expression of the anti-apoptotic protein Bcl2, thus blocking the activation of the apoptosis signal Caspase-3 and playing an anti-apoptotic role. Similarly, the results of the TUNEL assays showed that PHBA could reduce hippocampal neuronal apoptosis induced by brain injury in MCAO/R rats following stroke, which may be an important metabolic mechanism of PHBA in treating IS and improving the neurological dysfunction caused by cerebral I/R.

In summary, according to the results of histopathology and metabolomics analysis, the present study showed that PHBA protected against cerebral I/R injury. This may have been achieved via the activation of autophagy and by increasing the interaction between PSD-95 and AMPAR, which are related to synaptic plasticity in the hippocampus. Therefore, PHBA may serve as a promising therapeutic strategy for improving the prognosis of IS.

Acknowledgements

Not applicable.

Funding

The present study was supported by the National Natural Science Foundation of China (grant no. 81960733), the Xingdian Talent Support Program-Special for Young Talent (grant no. XDYC-QNRC-2022-0284) and the National Administration of Traditional Chinese Medicine High-level Key Discipline Construction Project 'Dai Medicine' and 'Dai Pharmacy'.

Availability of data and materials

The datasets used and/or analyzed during the current study are available from the corresponding author upon reasonable request. The relevant data sets have been submitted to the public database, <https://www.ebi.ac.uk/metabolights/editor/study/MTBLS7870>.

Authors' contributions

LY and XD designed the experiments. YL and XY conducted a preliminary analysis of animal experiments and metabolomics results. XY and XD revised the manuscript. XD and LY confirm the authenticity of all the raw data. All authors have read and approved the final manuscript.

Ethics approval and consent to participate

All animal experiments were approved by the Animal Ethics Committee of Yunnan University of Traditional Chinese Medicine (Kunming, China; approval no. R-062019039).

Patient consent for publication

Not applicable.

Competing interests

The authors declare that they have no competing interests.

References

1. No authors listed: Corrigendum to: World stroke organization (WSO): Global stroke fact sheet 2022. *Int J Stroke* 17: 478, 2022.
2. Wu MY, Yiang GT, Liao WT, Tsai AP, Cheng YL, Cheng PW, Li CY and Li CJ: Current mechanistic concepts in ischemia and reperfusion injury. *Cell Physiol Biochem* 46: 1650-1667, 2018.
3. Sun MS, Jin H, Sun X, Huang S, Zhang FL, Guo ZN and Yang Y: Free radical damage in ischemia-reperfusion injury: An obstacle in acute ischemic stroke after revascularization therapy. *Oxid Med Cell Longev* 2018: 3804979, 2018.
4. Messmer SJ, Salmeron KE, Frank JA, McLouth CJ, Lukins DE, Hammond TC, Lin AL, Fraser JF and Pennypacker KR: Extended middle cerebral artery occlusion (MCAO) model to mirror stroke patients undergoing thrombectomy. *Transl Stroke Res* 13: 604-615, 2022.
5. Ha JH, Lee DU, Lee JT, Kim JS, Yong CS, Kim JA, Ha JS and Huh K: 4-Hydroxybenzaldehyde from *Gastrodia elata* Blume is active in the antioxidation and GABAergic neuromodulation of the rat brain. *J Ethnopharmacol* 73: 329-333, 2000.
6. He F, Duan X, Dai R, Wang W, Yang C and Lin Q: Protective effects of ethyl acetate extraction from *Gastrodia elata* blume on blood-brain barrier in focal cerebral ischemia reperfusion. *Afr J Tradit Complement Altern Med* 13: 199-209, 2016.
7. Zhu YP, Li X, Du Y, Zhang L, Ran L and Zhou NN: Protective effect and mechanism of p-hydroxybenzaldehyde on blood-brain barrier. *Zhongguo Zhong Yao Za Zhi* 43: 1021-1027, 2018 (In Chinese).
8. Kim HJ, Hwang IK and Won MH: Vanillin, 4-hydroxybenzyl aldehyde and 4-hydroxybenzyl alcohol prevent hippocampal CA1 cell death following global ischemia. *Brain Res* 1181: 130-141, 2007.
9. Feng J, Yang JG, Yang QY, Xu Y and He F: Pharmacokinetics of metabolites of p-hydroxybenzaldehyde in rats. *China pharmaceuticals* 29: 9-12, 2020 (In Chinese).
10. Xiao T, Yang L, Chen P and Duan X: Para-hydroxybenzaldehyde against transient focal cerebral ischemia in rats via mitochondrial preservation. *Exp Ther Med* 24: 716, 2022.

11. Luo Y, Chen P, Yang L and Duan X: Metabolomic analysis and pharmacological validation of the cerebral protective effect of 3,4-dihydroxybenzaldehyde on cerebral ischemia-reperfusion injury. *Mol Med Rep* 27: 9, 2023.
12. Ramana P, Adams E, Augustijns P and Van Schepdael A: Metabonomics and drug development. *Methods Mol Biol* 1277: 195-207, 2015.
13. Wu Z, Qian S, Zhao L, Zhang Z, Song C, Chen L, Gao H and Zhu W: Metabonomics-based study of the potential interventional effects of Xiao-Xu-Ming Decoction on cerebral ischemia/reperfusion rats. *J Ethnopharmacol* 295: 115379, 2022.
14. Wang D, Wang Q, Chen R, Yang S, Li Z and Feng Y: Exploring the effects of *Gastrodia elata* Blume on the treatment of cerebral ischemia-reperfusion injury using UPLC-Q/TOF-MS-based plasma metabolomics. *Food Funct* 10: 7204-7215, 2019.
15. Zhang P, Huang Z, Yan HQ, Su LL, Gui YK, Lv HX, Zhu B and Li T: Improvement of the suture-occluded method in rat models of focal cerebral ischemia-reperfusion. *Exp Ther Med* 7: 657-662, 2014.
16. National Research Council (US) Committee for the Update of the Guide for the Care and Use of Laboratory Animals: Guide for the care and use of laboratory animals. 8th edition. Washington (DC): National Academies Press (US), 2011.
17. Liu J, Yang L, Niu Y, Su C, Wang Y, Ren R, Chen J and Ma X: Potential therapeutic effects of Mi-Jian-Chang-Pu Decoction on neurochemical and metabolic changes of cerebral ischemia-reperfusion injury in rats. *Oxid Med Cell Longev* 2022: 7319563, 2022.
18. Li H, Peng D, Zhang SJ, Zhang Y, Wang Q and Guan L: Buyang Huanwu Decoction promotes neurogenesis via sirtuin 1/autophagy pathway in a cerebral ischemia model. *Mol Med Rep* 24: 791, 2021.
19. Tsugawa H, Cajka T, Kind T, Ma Y, Higgins B, Ikeda K, Kanazawa M, VanderGheynst J, Fiehn O and Arita M: MS-DIAL: Data-independent MS/MS deconvolution for comprehensive metabolome analysis. *Nat Methods* 12: 523-526, 2015.
20. Heinemann J: Cluster analysis of untargeted metabolomic experiments. *Methods Mol Biol* 1859: 275-285, 2019.
21. Liu S, Xie X, Lei H, Zou B and Xie L: Identification of key circRNAs/lncRNAs/miRNAs/mRNAs and pathways in preclampsia using bioinformatics analysis. *Med Sci Monit* 25: 1679-1693, 2019.
22. Sandholm N, Van Zuydam N, Ahlqvist E, Juliusdottir T, Deshmukh HA, Rayner NW, Di Camillo B, Forsblom C, Fadista J, Ziemek D, *et al*: The genetic landscape of renal complications in type 1 diabetes. *J Am Soc Nephrol* 28: 557-574, 2017.
23. Kumar V, Spangenberg O and Konrad M: Cloning of the guanylate kinase homologues AGK-1 and AGK-2 from *Arabidopsis thaliana* and characterization of AGK-1. *Eur J Biochem* 267: 606-615, 2000.
24. Yan BC, Park JH, Ahn JH, Lee JC, Won MH and Kang JJ: Postsynaptic density protein (PSD)-95 expression is markedly decreased in the hippocampal CA1 region after experimental ischemia-reperfusion injury. *J Neurol Sci* 330: 111-116, 2013.
25. Simonini MV, Camargo LM, Dong E, Maloku E, Veldic M, Costa E and Guidotti A: The benzamide MS-275 is a potent, long-lasting brain region-selective inhibitor of histone deacetylases. *Proc Natl Acad Sci USA* 103: 1587-1592, 2006.
26. Kumaran D, Udayabanu M, Nair RU, R A and Katyal A: Benzamide protects delayed neuronal death and behavioural impairment in a mouse model of global cerebral ischemia. *Behav Brain Res* 192: 178-184, 2008.
27. Geenen S, Guallar-Hoyas C, Michopoulos F, Kenna JG, Kolaja KL, Westerhoff HV, Thomas P and Wilson ID: HPLC-MS/MS methods for the quantitative analysis of 5-oxoproline (pyroglutamate) in rat plasma and hepatic cell line culture medium. *J Pharm Biomed Anal* 56: 655-663, 2011.
28. Jiang Z, Sun J, Liang Q, Cai Y, Li S, Huang Y, Wang Y and Luo G: A metabonomic approach applied to predict patients with cerebral infarction. *Talanta* 84: 298-304, 2011.
29. Deery DJ and Taylor KW: Effect of phenylpyruvate on enzymes involved in fatty acid synthesis in rat brain. *Biochem J* 134: 557-563, 1973.
30. Jiang T, Jiao J, Shang J, Bi L, Wang H, Zhang C, Wu H, Cui Y, Wang P and Liu X: The differences of metabolites in different parts of the brain induced by shuxuetong injection against cerebral ischemia-reperfusion and its corresponding mechanism. *Evid Based Complement Alternat Med* 2022: 9465095, 2022.
31. Du C, Cao S, Shi X, Nie X, Zheng J, Deng Y, Ruan L, Peng D and Sun M: Genetic and biochemical characterization of a gene operon for trans-aconitic acid, a novel nematicide from *Bacillus thuringiensis*. *J Biol Chem* 292: 3517-3530, 2017.
32. Zhang C, Ling CL, Pang L, Wang Q, Liu JX, Wang BS, Liang JM, Guo YZ, Qin J and Wang JX: Direct macro-molecular drug delivery to cerebral ischemia area using neutrophil-mediated nanoparticles. *Theranostics* 7: 3260-3275, 2017.
33. Chen XL, Su SL, Liu R, Qian DW, Chen LL, Qiu LP and Duan JA: Chemical constituents and pharmacological action of bile acids from animal: A review. *Zhongguo Zhong Yao Za Zhi* 46: 4898-4906, 2021 (In Chinese).
34. Li C, Wang X, Yan J, Cheng F, Ma X, Chen C, Wang W and Wang Q: Cholic acid protects in vitro neurovascular units against oxygen and glucose deprivation-induced injury through the BDNF-TrkB signaling pathway. *Oxid Med Cell Longev* 2020: 1201624, 2020.
35. Quinn M, McMillin M, Galindo C, Frampton G, Pae HY and DeMorrow S: Bile acids permeabilize the blood brain barrier after bile duct ligation in rats via Rac1-dependent mechanisms. *Dig Liver Dis* 46: 527-534, 2014.
36. Menni C, Graham D, Kastenmüller G, Alharbi NH, Alsanosi SM, McBride M, Mangino M, Titcombe P, Shin SY, Psatha M, *et al*: Metabolomic identification of a novel pathway of blood pressure regulation involving hexadecanedioate. *Hypertension* 66: 422-429, 2015.
37. Sun D, Tiedt S, Yu B, Jian X, Gottesman RF, Mosley TH, Boerwinkle E, Dichgans M and Fornage M: A prospective study of serum metabolites and risk of ischemic stroke. *Neurology* 92: e1890-e1898, 2019.
38. Dong Y and Li HF: Research status of inherited disorders of metal metabolism in nervous system and the challenges faced. *Chin J Pract Intern Med* 42: 278-282, 2022.
39. Mendez NV, Wharton JA, Leclerc JL, Blackburn SL, Douglas-Escobar MV, Weiss MD, Seubert CN and Doré S: Clinical implications of bilirubin-associated neuroprotection and neurotoxicity. *Int J Clin Anesthesiol* 1: 1013, 2013.
40. Amin SB, Smith T and Timler G: Developmental influence of unconjugated hyperbilirubinemia and neurobehavioral disorders. *Pediatr Res* 85: 191-197, 2019.
41. Kurzepa J, Bielewicz J, Stelmasiak Z and Bartosik-Psujek H: Serum bilirubin and uric acid levels as the bad prognostic factors in the ischemic stroke. *Int J Neurosci* 119: 2243-2249, 2009.
42. Siebert H, Engelke S, Maruschak B and Brück W: Concentration-dependent effects of the esterase inhibitor BNPP on macrophage migration and myelin phagocytosis. *Brain Res* 916: 159-164, 2001.
43. Batirel HF, Aktan S, Aykut C, Yeğen BC and Coşkun T: The effect of aqueous garlic extract on the levels of arachidonic acid metabolites (leukotriene C4 and prostaglandin E2) in rat fore-brain after ischemia-reperfusion injury. *Prostaglandins Leukot Essent Fatty Acids* 54: 289-292, 1996.
44. Rao AM, Hatcher JF, Kindy MS and Dempsey RJ: Arachidonic acid and leukotriene C4: Role in transient cerebral ischemia of gerbils. *Neurochem Res* 24: 1225-1232, 1999.
45. Nguyen BT and Sadée W: Compartmentation of guanine nucleotide precursors for DNA synthesis. *Biochem J* 234: 263-269, 1986.
46. Kim E and Sheng M: PDZ domain proteins of synapses. *Nat Rev Neurosci* 5: 771-781, 2004.
47. Buonarati OR, Hammes EA, Watson JF, Greger IH and Hell JW: Mechanisms of postsynaptic localization of AMPA-type glutamate receptors and their regulation during long-term potentiation. *Sci Signal* 12: eaar6889, 2019.
48. Mardones MD, Jorquera PV, Herrera-Soto A, Ampuero E, Bustos FJ, van Zundert B and Varela-Nallar L: PSD95 regulates morphological development of adult-born granule neurons in the mouse hippocampus. *J Chem Neuroanat* 98: 117-123, 2019.
49. Poels J, Spasić MR, Callaerts P and Norga KK: An appetite for destruction: From self-eating to cell cannibalism as a neuronal survival strategy. *Autophagy* 8: 1401-1403, 2012.
50. Overhoff M, De Bruyckere E and Kononenko NL: Mechanisms of neuronal survival safeguarded by endocytosis and autophagy. *J Neurochem* 157: 263-296, 2021.
51. Lou G, Palikaras K, Lautrup S, Scheibye-Knudsen M, Tavernarakis N and Fang EF: Mitophagy and neuroprotection. *Trends Mol Med* 26: 8-20, 2020.

52. Jiang T, Yu JT, Zhu XC, Zhang QQ, Tan MS, Cao L, Wang HF, Shi JQ, Gao L, Qin H, *et al*: Ischemic preconditioning provides neuroprotection by induction of AMP-activated protein kinase-dependent autophagy in a rat model of ischemic stroke. *Mol Neurobiol* 51: 220-229, 2015.
53. Dai SH, Chen T, Li X, Yue KY, Luo P, Yang LK, Zhu J, Wang YH, Fei Z and Jiang XF: Sirt3 confers protection against neuronal ischemia by inducing autophagy: Involvement of the AMPK-mTOR pathway. *Free Radic Biol Med* 108: 345-353, 2017.
54. Tran S, Fairlie WD and Lee EF: BECLIN1: Protein structure, function and regulation. *Cells* 10: 1522, 2021.
55. Lamark T, Svenning S and Johansen T: Regulation of selective autophagy: The p62/SQSTM1 paradigm. *Essays Biochem* 61: 609-624, 2017.
56. Ritzel RM, Li Y, He J, Khan N, Doran SJ, Faden AI and Wu J: Sustained neuronal and microglial alterations are associated with diverse neurobehavioral dysfunction long after experimental brain injury. *Neurobiol Dis* 136: 104713, 2020.
57. Li Z, Xiao G, Wang H, He S and Zhu Y: A preparation of Ginkgo biloba L. leaves extract inhibits the apoptosis of hippocampal neurons in post-stroke mice via regulating the expression of Bax/Bcl-2 and caspase-3. *J Ethnopharmacol* 280: 114481, 2021.



Copyright © 2023 Yu et al. This work is licensed under a Creative Commons Attribution-NonCommercial-NoDerivatives 4.0 International (CC BY-NC-ND 4.0) License.